# RSC Advances

ROYAL SOCIETY OF CHEMISTRY

www.rsc.org/advances

# Journal Name

## ARTICLE

# Aggregation and thermal gelation of N-isopropylacrylamide based cucurbit[7]uril side-chain polypseudorotaxanes with low pseudorotaxane content

Hao Chen,[ab] Haili Ma,[ab] Yu Yuan Chieng,[c] Shengzhen Hou,[ab] Xu Li[*c] and Yebang Tan[*ab]

N-isopropylacrylamide (NIPAA) based cucurbit[7]uril (CB[7]) side-chain polypseudorotaxanes with low pseudorotaxane content were designed with the intention to emulate rod-coil block copolymers. In the polypseudorotaxanes, CB[7] pseudorotaxane units acted as rigid "rod segments" and the remaining polymer chain acted as the "soft-coils". The length of soft-coil segments, which determines aggregation behavior, can be easily tuned by change the CB[7] pseudorotaxane content. The polypseudorotaxanes with much lower pseudorotaxane content demonstrate unique aggregation behavior, with a strong tendency for aggregation and thermal gelation. Their aggregation behavior and the formed hydrogels were studied with dynamic light scattering (DLS), and rheological and microscopic experiments. The mechanism of the unique aggregation behavior was also investigated.

## 1. Introduction

Poly(pseudo)rotaxanes are a special class of polymers incorporated with (pseudo)rotaxane moieties.[1-4] They can be divided into two types: namely main-chain poly(pseudo)rotaxanes and side-chain poly(pseudo)rotaxanes, depending on the (pseudo)rotaxane moieties' location. Poly(pseudo)rotaxanes have been intensively studied due to their unique structures and properties, which endows them with the ability to construct intelligent materials.[5-10] Understanding the relationship between the structures and properties of poly(pseudo)rotaxanes is critical for the advancement of the field.

Cucurbiturils (CBs) are a series of macrocyclic host molecules which consist of methylene bridged glycolurils.[11-15] Their high binding affinity, high binding selectivity, volumetric and rigid structure have been explored in various fields.[16-27] Numerous CB based poly(pseudo)rotaxanes have been constructed, depending on eminent binding properties of CBs.[9,28-39] Among them, construction of CB based side-chain poly(pseudo)rotaxanes through (co)polymerization is well established.[34-39] CB based side-chain polypseudorotaxanes were firstly reported by Tan et al.;[36] here the polypseudorotaxanes were synthesized through the polymerization of protonated diaminobutane based monomers to construct the polymer backbones, followed by threading CB[6] on the side-chain of the polymers. These polypseudorotaxanes displayed higher conformational rigidity than the pristine polymer due to the large size of CB[6]. Subsequently Ritter et al. and Nakamoto et al. reported polypseudorotaxanes with N-isopropyacrylamide (NIPAA) based copolymer backbones which threaded with CB[6] and CB[7] respectively.[37,38] The formation of polypseudorotaxanes changes the aggregation behavior of pristine copolymers. These polypseudorotaxanes demonstrated an increase in low critical solution temperature (LCST) and loss of turbidity. In our previous study, polypseudorotaxanes with movable CB[7] rings were synthesized.[39] The size of the polypseudorotaxanes was found to increase following the loading of CB[7] onto the polymer backbone. To the best of our knowledge, there has been no CB based side-chain polypseudorotaxanes with less than 5 mol% pseudorotaxane unit reported until now.

The concept of rod-coil block copolymers is used to describe copolymers with rigid rod-segments and flexible coil blocks; and they are known for their fascinating aggregation and self-assembling behavior.[40,41] Under certain condition, even if the length of the segments is short (less than 2000 Da), they still have a profound effect on self-assembling of the copolymers.[42,43] Since CBs are volumetric and rigid, in certain polypseudorotaxanes they could work as the "rod-segment" (one CB[7] pseodorotaxane unit have a molecular weight of around 1300 Da) and segregate the rest polymer chain as soft-coil segments. Through tuning the loading amount of CBs, the
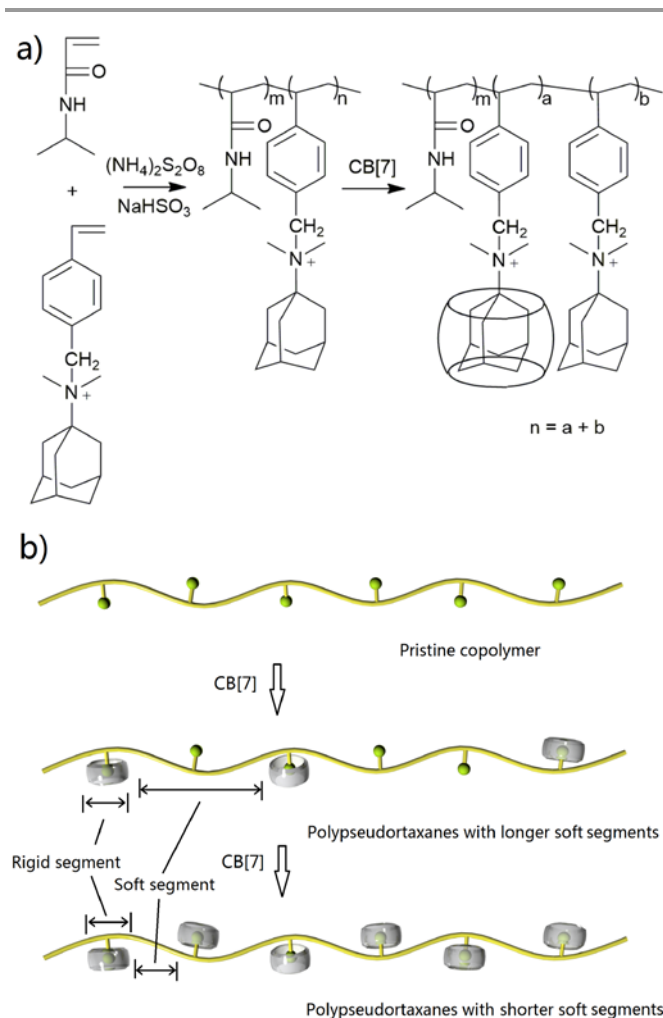
**Scheme 1** a) Preparation procedure of the NIPAA based CB[7] polypseudorotaxanes and b) tuning length of soft segments in the polypseudorotaxanes by changing the loading amount of CB[7].

length of the soft-coil segments, and thus the aggregation behaviour of the system, can be controlled facilely. Based on this idea, NIPAA based CB[7] side-chain polypseudorotaxanes with low pseudorotaxane content, which endow the polypseudorotaxanes much longer soft-coils, were prepared and studied. These polypseudorotaxanes demonstrate unique aggregation behavior, with a strong tendency of aggregation and thermal gelation. The properties of these polypseudorotaxanes were evaluated by employing dynamic light scattering (DLS), and rheology and microscopy. The mechanism of their unique aggregation behavior was investigated.

## 2. Experimental

### 2.1 Materials

CB[7] was synthesized following literature procedure.[12] Amantadine hydrochloride, 4-vinylbenzyl chloride and NIPAA were purchased from J&K Scientific. Dichloromethane, sodium hydroxide, methanol, diethyl ether and hydrochloric acid were obtained from Sinopharm Chemical Reagent Co., Ltd.. Synthesis procedure of monomer N-adamantyl-N-(4-vinyl benzyl)-N,N-dimethyl ammonium chloride (AD4VBDMA) can be found in supplementary information.

### 2.2 Synthesis of the pristine copolymer

The pristine copolymer of the polypseudorotaxanes was synthesized through redox-initiated polymerization. AD4VBDMA (1.494 g, 0.0045 mol) and NIPAA (14.6 g, 0.129 mol) were dissolved in 200 mL deionized water. The solution was degassed under vacuum and purged with nitrogen for three cycles. $(NH_4)_2S_2O_8$ solution containing 0.0584 g ($2.56 \times 10^{-4}$ mol) solute was injected into the monomer solution followed by $NaHSO_3$ solution containing 0.021 g ($2.05 \times 10^{-4}$ mol) solute. The solution was allowed to stand at 25 °C for 5 hours and gradually heated to 30 °C for another 5 hours. After the reaction, this solution was dialyzed in deionized water using semi-permeable membrane (MWCO: 8000 – 14000) for three days to remove unreacted monomers and impurities. This polymer solution was further concentrated to 92 g with concentration of 14.8 w/w% under vacuum. The yield of polymer is 84.6 %.

### 2.3 Preparation of NIPAA based CB[7] polypseudorotaxanes

The NIPAA based CB[7] polypseudorotaxanes with various composition and concentration is prepared by mixing the pristine copolymer stock solution with quantitative CB[7] suspension and pure water. The preparation of a 5 wt% polypseudorotaxane (with pseudorotaxane content R = 1.5 mol%) solution was used as an example. The stock solution (2.6059 g) was transferred into an empty vial. In order to achieve the desired concentration of 5 wt%, 4.395 g pure water was added firstly followed by 1.590 g CB[7] suspension (7.395 wt%). The mixture was mixed with vortex (1500 rpm, 30 s).

### 2.4 Instruments

Nuclear Magnetic Resonance (NMR) tests were conducted by using a Bruker Avance 400 NMR spectrometer at 298 K. Mass spectrometry was tested on Agilent 6520 accurate mass Q-TOF. The turbidity of copolymers with different amount of CB[7] were tested on a Persee TU1901 ultraviolet spectrophotometer. Multi-angle laser light scattering (MALLS) and dynamic light scattering (DLS) measurements were performed on the Wyatt Technology DAWN HELEOS 18 angle light scattering detector (Ga As laser, 658 nm, 40 mW). Low polymer concentration of 0.01 mg mL$^{-1}$ was used for DLS experiment to ensure negligible multiple scattering.

### 2.5 Rheological study

Rheological properties were measured using a HAAKE MARS Ⅲ rheometer. Steady-shear and strain-dependent oscillatory rheology of polymer solutions were measured using a CC27 DG Ti geometry at 25 °C. Gelation process and hydrogel properties were measured using a C60/1° Ti L geometry. The gelation process was tested under CD-auto strain mode with γ = 0.02. The strain-dependent oscillatory rheology and frequency-

dependent oscillatory rheology of hydrogels were tested at 1 Hz and γ = 0.02 at 45 °C, respectively.

### 2.6 Microscopic observations

Optical and polarizing microscopic images were obtained using an Olympus BX-51 polarizing microscope with Linkam THMSE 600. The copolymer solutions were dropped on microscope slide and then spread evenly by cover glass at room temperature. These samples were then gradually heated to 45 °C on heating stage and the microscopic images can be obtained *in-situ*.

Transmission Electron Microscopy (TEM) images were taken using a JEOL JEM-2100 F with accelerating voltage at 200 kV. The solution of the pristine copolymer (2 wt%) was firstly heated to 45 °C to get a turbid suspension. The suspension was then dispersed in a large quantity of water (about 100 times of initial volume) at 45 °C and coated on a copper grid. The copper grid was dried at 45 °C for 24 hours before observing with TEM.

## 3. Results and discussion

### 3.1 NIPAA based CB[7] polypseudorotaxanes

The host-guest interaction between CB[7] and amantadine derivatives is extremely strong, with the binding entropies and binding affinities of around 20 kcal mol$^{-1}$ and over $10^{10}$ M$^{-1}$ respectively.[16-19] In order to construct stable NIPAA based polypseudorotaxanes, AD4VBDMA, which is derived from amantadine, was designed and copolymerized with NIPAA. The copolymerization was conducted through redox-initiated polymerization. Unreacted monomers and impurities were removed through dialysis in deionized water. The molecular weight of the copolymer was measured by multi-angle laser light scattering (MALLS) and found to be $(2.20 \pm 0.35) \times 10^5$ g mol$^{-1}$. The molar composition of the copolymer was found to be 3.0/97.0 for AD4VBDMA/NIPAA units as determined by $^1$H

NMR. The polypseudorotaxanes with different pseudorotaxane content could form spontaneously after mixing of the pristine copolymer solution with quantitative amount of CB[7].

NMR analysis is a universal method for characterizing the supramolecular interactions. For CB based host-guest complexes, the atoms on guest molecule are shielded and exerted a different chemical shift due to the encapsulation of guest molecule inside the CB cavity.[44] As shown in **Fig. 1**, after mixing AD4VBDMA with CB[7], a distinct change in the spectrum especially on its adamantyl group was observed, indicating that the CB[7] is threaded on its adamantyl part. This is in accordance with the fact that CB[7] exerts a high binding affinity with amantadine derivatives.[16-19] The signal of CB[7] also changed significantly after the formation of the host-guest complex.[45] The signal of its methylene hydrogen was split into double doublet (peaks at 5.69 and 4.14 ppm for **Fig. 1c**). When the solution of the pristine copolymer was mixed with CB[7], the signals of adamantyl moiety of the copolymer at 2.36 and 2.20 ppm disappeared (see **Fig. 1a**). It is postulated that these signals shift to up-field and overlap with NIPPA peaks based on the spectrum of AD4VBDMA·CB[7] host-guest complex. Moreover, the methylene hydrogen on CB[7] was also split and broadened (peaks at 5.74 and 4.17 ppm for **Fig. 1a**). These evidence suggest that the CB[7] has threaded onto the adamantyl groups of the copolymer and formed the desired polypseudorotaxane.

### 3.2 Aggregation behavior of the NIPAA based CB[7] polypseudorotaxanes

DLS is an effective method to study the aggregation behavior of macromolecules in solution. As shown in **Fig. 2a**, the hydrodynamic radius of the pristine copolymer increases drastically after addition of CB[7]. The increase on hydrodynamic radius during the formation of polypseudorotaxanes has been previously reported by our group, which can be attributed to the increase on the size of the polypseudorotaxanes induced by increase in rigidity.[39] It should be noted that the increase in that situation was relatively small.
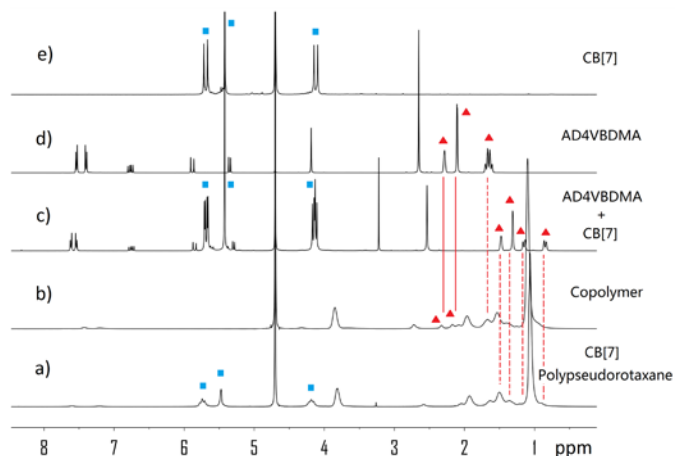


**Fig. 1** $^1$H NMR spectra of a) polypseudorotaxane (with 3 mol% pseudorotaxane units); b) pristine copolymer; c) AD4VBDMA with 1 equiv CB[7]; d) AD4VBDMA; e) CB[7] at 298 K in D$_2$O. (Red triangles mark the peaks corresponding to adamantyl group and blue squares represent the peaks of CB[7].)
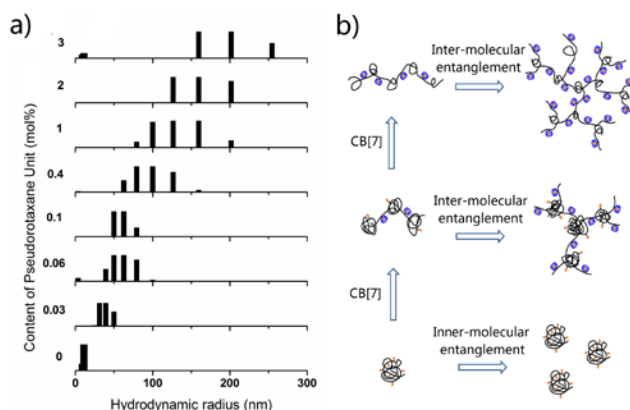


**Fig. 2** a) Hydrodynamic radius of the polypseudorotaxanes with increasing pseudorotaxane content and b) Schematic description of the aggregation behavior of the polypseudorotaxanes with different pseudorotaxane content.

The largest amplitude is from 18 to 30 nm with 100 mol% double rings pseudorotaxane units formed. In this work, however, the increase amplitude of the hydrodynamic radius during the formation of polypseudorotaxanes is much larger. For instance, when 2 mol% CB[7] (molar ratio of CB[7] *versus* monomer repeat units) was loaded to pristine copolymer, the hydrodynamic radius increased from 9 to 150 nm, which indicates the aggregation of the polypseudorotaxanes. Based on the rigid-soft alternate structure of the polypseudorotaxanes, the drastic increase in the hydrodynamic radius was explained by the following mechanism (see **Fig. 2b**): unlike the increase on rigidity across whole polymer chain of polypseudorotaxanes with high pseudorotaxane content,[34-39] with these NIPAA based CB[7] polypseudorotaxanes, due to their low pseudorotaxane content, the rigid CB[7] pseudorotaxane segments only partially hinder the entanglement of polymer chain, making the polypseudorotaxane structure more outstretched. The remaining soft segments of the polypseudorotaxanes acted as soft-coils and are still capable of entangling. The extension on the structure makes the entanglement of these soft-coils occur in a more inter-molecular manner and therefore results in the aggregation of the polypseudorotaxanes. Under a certain range, the polypseudorotaxanes have long enough soft-coil segments to entangle. Increase on the pseudorotaxane content within this range will help create more soft-coil segments which promotes the formation of larger aggregates of the polypseudorotaxanes.

Rheological study of the polypseudorotaxanes was also conducted. The steady-shear results of polypseudorotaxanes with different amounts of CB[7] pseudorotaxane unit are shown in **Fig. 3**. Shear-thinning behavior of solutions indicates the disentanglement of polymer chain. The solutions of the polypseudorotaxanes display much higher viscosity and more remarkable shear-thinning behavior compared to the solution of their pristine copolymer. This result is consistent with DLS results, which show that the polypseudorotaxanes demonstrate strong tendency for aggregation. Interestingly, the polypseudorotaxane with 2 mol% pseudorotaxane units rather than the one with 3 mol% demonstrated the highest viscosity at a low shear rate region. This behavior can also been explained by the model given in **Fig. 2b**：as the content of rigid CB[7] pseudorotaxane units increase, the amount of soft-coils increase. But the average length of soft-coils decreases. The increase of
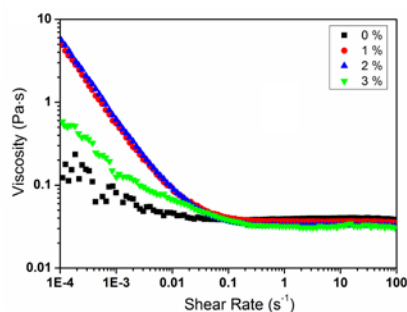
the amount of soft-coils brings more entanglement sites while the decrease on length weaken the entanglement strength. The polypseudorotaxane with 2 mol% pseudorotaxane units shows the highest viscosity is the result of the competition of these two effects.

Under a high shear rate (above 0.1 s$^{-1}$), the pristine copolymer and the polypseudorotaxanes were fully disentangled as indicated by the low viscosity plateau. In this region the viscosity of the pristine copolymer is the highest and the viscosities of polypseudorotaxanes decrease with increasing pseudorotaxane content. This can be attributed to the blocking of the inter-chain interaction by the CB[7]'s bulky structure, which indicates that CB[7] works as a structure regulator rather than a supramolecular cross-linker.[35]

### 3.3 Thermally gelling of the NIPAA based CB[7] polypseudorotaxanes

Vial inclination method is a convenient, qualitative and intuitive approach to study the thermal gelation process. As illustrated in **Fig. 4a**, when heated up to 45 °C, the solution of 4 wt% pristine copolymer turned to a turbid suspension. It is important to note that the pristine copolymer solution with even 10 wt% cannot form a hydrogel. On the contrary, when a 4 wt% solution of the polypseudorotaxane containing 2 mol% CB[7] pseudorotaxane units was heated to 45 °C, it immediately formed an opaque hydrogel. The hydrogel is extremely stable and cannot be destroyed even with violent shake. Further, no obvious syneresis of the hydrogel was observed after stored at 45 °C for 2 days.

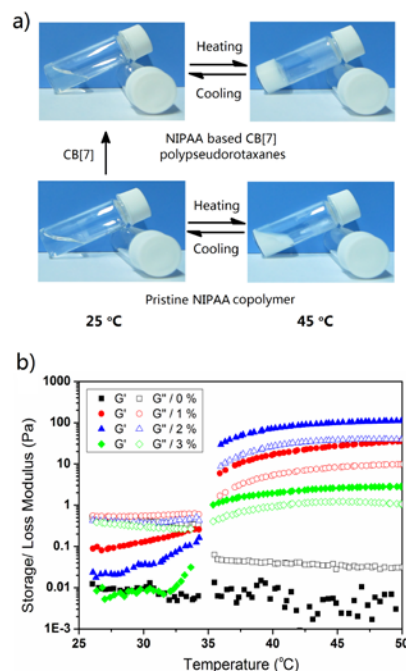Temperature dependent oscillation experiments were



**Fig. 4** Thermally responsive studies of the pristine copolymer and the polypseudorotaxanes through a) vial inclination observation and b) temperature dependent oscillatory rheological experiments.



**Fig. 3** Steady-shear results of the polypseudorotaxanes (4 wt%) with different CB[7] pseudorotaxane content at 25 °C.

carried out in order to have a better understanding on the gelation process of the hydrogels (**Fig. 4b**). For all samples, the loss modulus (G'') is dominant over the storage modulus (G') below 34 °C, indicating that all of them behave like a fluid at this temperature range. When the temperature approaches 34 °C, a sharp transition was observed with all samples. While the moduli of the pristine copolymer solution decrease, the moduli of all the polypseudorotaxane solutions increase drastically with G' surpassing G'', demonstrating that the formation of hydrogels of the polypseudorotaxane solutions. Turbidity measurement shows that these polymers have same LCST at 34 °C (**Fig. S1**). Even though the hydrophobic interaction of PNIPAA segments increases at high temperature, the pristine copolymer cannot form a hydrogel. The hydrogel formed by polypseudorotaxane containing 2 mol% CB[7] pseudorotaxane units demonstrates highest mechanical strength and followed by polypseudorotaxane containing 1 and 3 mol% CB[7] pseudorotaxane units. The same trend between hydrogels' mechanical strength and corresponding polypseudorotaxanes' viscosity indicate that the aggregation of these polypseudorotaxanes induces the formation of hydrogels.

### 3.4 Structure of the thermally reversible hydrogels

In order to have a better understanding on the gelation mechanism and the relationship between CB[7] pseudorotaxane content and the aggregation behavior, the structure of hydrogels were studied. *In-situ* optical microscopic images are shown in **Fig. 5**: here it can be seen that the morphology of aggregation changes with increasing CB[7] pseudorotaxane content. The morphology of aggregates is globular for pristine copolymer. By increasing pseudorotaxane content to 1 mol%, the morphology becomes more outstretched and displays a trend to form a network. With further addition of CB[7] to 2 mol%, the aggregates forms an integrated network. However, with pseudorotaxane content of 3 mol%, the integrated network is destroyed and become fragmented. This confirm that the
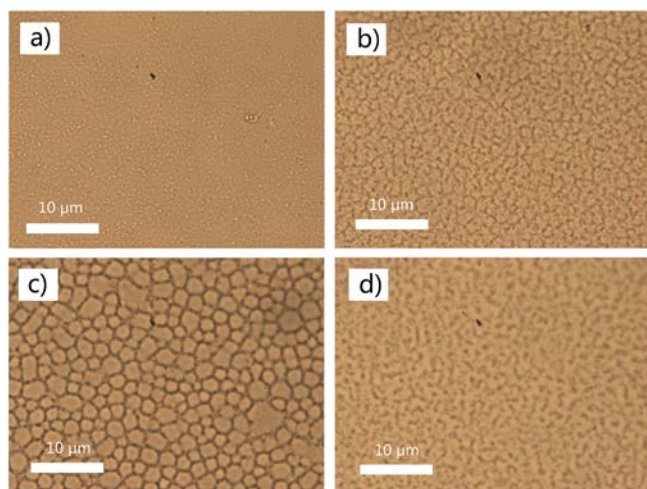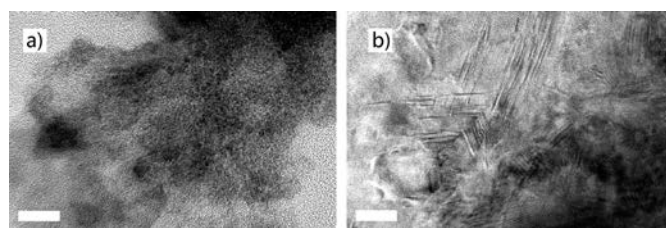


**Fig. 6** TEM images of microstructure of the aggregates of a) the pristine copolymer and b) the polypseudorotaxane with 2 mol% pseudorotaxane units. The length of scale bars is 20 nm.

aggregation of polypseudorotaxanes below LCST have a great effect on the self-assembling above LCST and finally induces the formation of hydrogels. The difference in the structure of hydrogels reflects in their difference of their mechanical strength as higher skeleton integrity corresponding to higher mechanical strength. Another interesting phenomenon is the skeleton of the hydrogel can be observed by polarizing optical microscope (see **Fig. S2**), indicating that there is finely ordered sub-structure in the hydrogel skeleton.

Transmission electron microscope (TEM) was used to investigate the fine structure of the hydrogels' skeleton. As shown in **Fig. 6**, the morphology for the pristine copolymer aggregates is amorphous while oriented micro domains could be found in the sample of the polypseudorotaxane with 2 mol% pseudorotaxane units. The oriented micro domains are probably formed due to the self-assembling of rigid segments of CB[7] pseudorotaxane units and soft-coils of the remaining PNIPAA segments. The relatively low regularity of the micro domains is attributed to the high polydispersity of the rigid and soft segments. The oriented domains are expected to reinforce the skeleton of hydrogels and stabilize the hydrogels.

### 3.5 Rheological studies of the hydrogels



**Fig. 7** Oscillatory rheological analysis of the hydrogels at 45 °C. a) Storage and loss moduli of strain-amplitude sweep obtained at 1 Hz; b) Storage and loss moduli of frequency sweep obtained at 2 % strain; c) Summary of moduli and tangent phase angle (tan δ) versus the content pseudorotaxane units; d) Summary of moduli of hydrogels with different polypseudorotaxane concentration.



**Fig. 5** *In-situ* optical microscopic images of a) the pristine copolymer; b) - d) polypseudorotaxanes with 1, 2 and 3 mol % pseudorotaxane units at 45 °C (5 wt%).
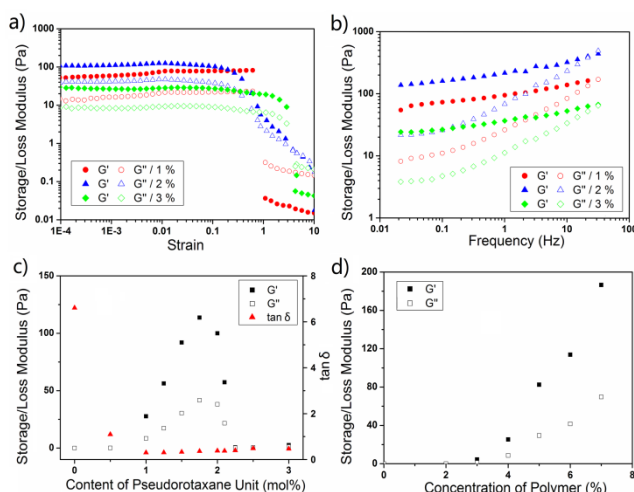
The performance of hydrogels was further studied by employing oscillatory rheological methods. **Fig. 7a** depicts the moduli of hydrogels *versus* applied strain. The linear viscoelastic region (plateau region) where the moduli are independent of strain can therefore be identified. All the hydrogel samples display a wide linear viscoelastic region, indicating that the hydrogels are elastic. As described previously, the hydrogel formed by polypseudorotaxane with 2 mol% pseudorotaxane units demonstrates maximal mechanical strength, however it demonstrates the lowest breakdown amplitude. This phenomenon may be attributed to the integrated hydrogel network decreases the hydrogel's flexibility.

The frequency-dependent oscillatory rheology performed at linear viscoelastic region is shown in **Fig. 7b**. In brief, G' is dominant in the whole range of frequency showing the hydrogel intuition of these materials. There is no low-frequency terminal region observed in these plots, suggesting that the hydrogels have a very low relaxation rate. It is interesting to find that the increase rate of G'' is faster than G' up to an intersection point at around 20 Hz, which might be due to the micrometer scale porous structure of the hydrogels. As frequency increases, the water in the hydrogel structure is perturbed more frequently. Therefore more energy was dissipated in the hydrogel structure under higher frequency during the test. Thus G'', which is used to describe the loss of energy, increases faster than G'.

To study the relationship between pseudorotaxane content and mechanical property of hydrogels, a plot of moduli and phase angle (tan δ) *versus* molar ratio of pseudorotaxane unit is presented in **Fig. 7c**. It can be seen that tan δ decreases rapidly with increasing pseudorotaxane content before it reaches 0.5 mol%, indicating the trend of the formation of hydrogels. As the amount of pseudorotaxane content reaches 1 mol%, tan δ is around 0.4 followed by a slight increase with further increasing pseudorotaxane content. Although samples containing over than 1 mol% of pseudorotaxane units are in the hydrogel state, the moduli of these samples varies. The optimal ratio of pseudorotaxane units of polypseudorotaxane for the hydrogel to exert the highest mechanical property is between 1.5 - 2.0 mol%, specifically at 1.75 mol%.

Polymer concentration will also affect the properties of hydrogels. Optimal ratio of polypseudorotaxanes with 1.75 mol% of pseudorotaxane units, but at different polymer concentrations was investigated (see **Fig. 7d**). As expected, the moduli of hydrogel increase with increasing polymer concentration. The critical gelation concentration was detected at 3 wt%, which is at a low level among thermally reversible hydrogels.[46-51]

In addition, the thermal reversibility of the hydrogels was investigated through rheological study. **Fig. S3a** displays a "sol-to-gel" and "gel-to-sol" cycle of hydrogel formed at 5 wt % polypseudorotaxane with 1.75 mol% pseudorotaxane unit. Results reveal that the gelation temperature of the hydrogel is 34 °C. However, the de-gelation temperature was slightly lower at 32 °C, depicting hysteresis of the hydrogel. Similar hysteresis of thermal responsive hydrogels have been reported by others, and the hysteresis can be explained through an entropic point of view.[52] Statistically speaking the disorder degree of the hydrogels are much less than the solutions therefore the formation of the hydrogels is more difficult. The gelation temperature and strength of gel remained constant even after 20 gelation-degelation cycles (**Fig. S3b**), demonstrating that the hydrogel is highly reversible.

## 4. Conclusions

NIPAA based CB[7] polypseudorotaxanes with low pseudorotaxane content were designed and prepared. They demonstrate unique aggregation behavior – strong tendency for aggregation and thermally-induced gelation. The unique aggregation behavior can be attributed to the rigid-soft block structure of the polypseudorotaxanes. The rigid pseudorotaxane units tune the entanglement manner of the PNIPAA soft-coil segments and the entanglement of the soft-coil segments provides the force for aggregation. The aggregation of the polypseudorotaxanes induces the formation of hydrogels above their LCST. The amount of CB[7] pseudorotaxane units determines the amount and the length of the PNIPAA soft-coils. Higher amounts of the soft-coil segments offer more entanglement points while longer lengths offer stronger entanglement for each entanglement site. The competition between these two factors determines the strength of aggregation and further affects the structure and mechanical properties of the hydrogels. The hydrogels formed by the polypseudorotaxanes demonstrate features including sharp transition on temperature, stable performance on wide temperature range, no noticeable syneresis, tunable mechanical properties and low critical gelation concentration. The knowledge gained in this study will be helpful in the construction of smart materials.

## Acknowledgements

## Notes and references

[a]School of Chemistry and Chemical Engineering, Shandong University, Jinan 250100, People's Republic of China
[b]The Key Laboratory of Special Functional Aggregated Materials, Ministry of Education, Shandong University, Jinan 250100, People's Republic of China
[c]Institute of Materials Research and Engineering, Agency for Science, Technology and Research (A*STAR), 3 Research Link, Singapore 117602

1    F. Huang and H. W. Gibson, *Prog. Polym. Sci.*, 2005, **30**, 982.
2    A. Harada, Y. Takashima and H. Yamaguchi, *Chem. Soc. Rev.*, 2009, **38**, 875.
3    J. Li and X. J. Loh, *Adv. Drug Deliver. Rev.*, 2008, **60**, 1000.

4   F. Davis and S. Higson, Macrocycles: Construction, Chemistry and Nanotechnology Applications, 1st Edition, 2011 John Wiley & Sons, Ltd.

5   N. Kihara, K. Hinoue and T. Takata, *Macromolecules*, 2005, **38**, 223.

6   T. Kataoka, M. Kidowaki, C. Zhao, H. Minamikawa, T. Shimizu and K. Ito, *J. Phys. Chem. B*, 2006, **110**, 24377.

7   Y. Okumura and K. Ito, *Adv. Mater.*, 2001, **13**, 485.

8   A. B. Imran, K. Esaki, H. Gotoh, T. Seki, K. Ito, Y. Sakai and Y. Takeoka, *Nat. Commun.*, DOI: 10.1038/ncomms6124.

9   Y. Liu, J. Shi, Y. Chen and C.-F. Ke, *Angew. Chem. Int. Ed.*, 2008, **47**, 7293.

10  P. N. Taylor, M. J. O'Connell, L. A. McNeill, M. J. Hall, R. T. Aplin and H. L. Anderson, *Angew. Chem. Int. Ed.*, 2000, **39**, 3456.

11  J. Kim, I.-S. Jung, S.-Y. Kim, E. Lee, J.-K. Kang, S. Sakamoto, K. Yamaguchi and K. Kim, *J. Am. Chem. Soc.*, 2000, **122**, 540.

12  A. Day, A. P. Arnold, R. J. Blanch and B. Snushall, *J. Org. Chem.*, 2001, **66**, 8094.

13  J. W. Lee, S. Samal, N. Selvapalam, H.-J. Kim and K. Kim, *Acc. Chem. Res.*, 2003, **36**, 621.

14  J. Lagona, P. Mukhopadhyay, S. Chakrabarti and L. Isaacs, *Angew. Chem. Int. Ed.*, 2005, **44**, 4844.

15  E. Masson, X. Ling, R. Joseph, L. Kyeremeh-Mensah and X. Lu, *RSC Adv.*, 2012, **2**, 1213.

16  S. Liu, C. Ruspic, P. Mukhopadhyay, S. Chakrabarti, P. Y. Zavalij and L. Isaacs, *J. Am. Chem. Soc.*, 2005, **127**, 15959.

17  S. Moghaddam, C. Yang, M. Rekharsky, Y. H. Ko, K. Kim, Y. Inoue and M. K. Gilson, *J. Am. Chem. Soc.*, 2011, **133**, 3570.

18  M. V. Rekharsky, T. Mori, C. Yang, Y. H. Ko, N. Selvapalam, H. Kim, D. Sobransingh, A. E. Kaifer, S. Liu, L. Isaacs, W. Chen, S. Moghaddam, M. K. Gilson, K. Kim and Y. Inoue, *Proc. Natl. Acad. Sci. U.S.A.*, 2007, **104**, 20737.

19  L. Cao, M. Šekutor, P. Y. Zavalij, K. Mlinarić-Majerski, R. Glaser and L. Isaacs, *Angew. Chem. Int. Ed.*, 2014, **53**, 988.

20  S. W. Heo, T. S. Choi, K. M. Park, Y. H. Ko, S. B. Kim, K. Kim and H. I. Kim, *Anal. Chem.*, 2011, **83**, 7916.

21  I. Hwang, K. Baek, M. Jung, Y. Kim, K. M. Park, D.-W. Lee, N. Selvapalam and K. Kim, *J. Am. Chem. Soc.*, 2007, **129**, 4170.

22  X. Lu, and E. Masson, *Org. Lett.*, 2010, **12**, 2310.

23  N. Saleh, A. L. Koner and W. M. Nau, *Angew. Chem. Int. Ed.*, 2008, **47**, 5398.

24  T. A. Martyn, J. L. Moore, R. L. Halterman and W. T. Yip, *J. Am. Chem. Soc.*, 2007, **129**, 10338.

25  H. Yang, Z. Ma, Z. Wang and X. Zhang, *Polym. Chem.*, 2014, **5**, 1471.

26  E. A. Appel, X. J. Loh, S. T. Jones, F. Biedermann, C. A. Dreiss and O. A. Scherman, *J. Am. Chem. Soc.*, 2012, **134**, 11767.

27  Z. Huang, L. Yang, Y. Liu, Z. Wang, O. A. Scherman and X. Zhang, *Angew. Chem. Int. Ed.*, 2014, **53**, 5351.

28  D. Tuncel and J. H. G. Steinke, *Chem. Commun.*, 1999, 1509.

29  D. Tuncel, H. B. Tiftik and B. Salih, *J. Mater. Chem.*, 2006, **16**, 3291.

30  J. Kim, Y. Ahn, K. M. Park, D.-W. Lee and K. Kim, *Chem. Eur. J.*, 2010, **16**, 12168.

31  D. Tuncel and J. H. G. Steinke, *Macromolecules*, 2004, **37**, 288.

32  T. Ooya, D. Inoue, H. S. Choi, Y. Kobayashi, S. Loethen, D. H. Thompson, Y. H. Ko, K. Kim and N. Yui, *Org. Lett.*, 2006, **8**, 3159.

33  S. W. Choi, J. W. Lee, Y. H. Ko and K. Kim, *Macromolecules*, 2002, **35**, 3526.

34  Z.-S. Hou, Y.-B. Tan, K. Kim and Q.-F. Zhou, *Polymer*, 2006, **47**, 742.

35  Z. Hou, Y. Tan and Q. Zhou, *Polymer*, 2006, **47**, 5267.

36  Y. Tan, S. W. Choi, J. W. Lee, Y. H. Ko and K. Kim, *Macromolecules*, 2002, **35**, 7161.

37  S. W. Choi and H. Ritter, *Macromol. Rapid Commun.*, 2007, **28**, 101.

38  T. Ogoshi, K. Masuda, T. Yamagishi and Y. Nakamoto, *Macromolecules*, 2009, **42**, 8003.

39  H. Yang, J. Hao and Y. Tan, *J. Polym. Sci., Part A: Polym. Chem.*, 2011, **49**, 2138.

40  A. N. Semenov, S. V. Vasilenko, *Sov. Phys. JETP S. V.*, 1986, **63**, 70.

41  H.-A. Klok and S. Lecommandoux, *Adv. Mater.*, 2001, **13**, 1217.

42  S. A. Jenekhe and X. L. Chen, *Science*, 1999, **283**, 372.

43  S. I. Stupp, V. LeBonheur, K. Walker, L. S. Li, K. E. Huggins, M. Keser, A. Amstutz, *Science*, 1997, **276**, 384.

44  W. L. Mock and N.-Y. Shih, *J. Org. Chem.*, 1986, **51**, 4440.

45  H. Chen, H. Yang, W. Xu and Y. Tan, *RSC Adv.*, 2013, **3**, 13311.

46  B. Jeong, S. W. Kim and Y. H. Bae, *Adv. Drug Deliver. Rev.*, 2002, **54**, 37.

47  H.-H. Lin and Y.-L. Cheng, *Macromolecules*, 2001, **34**, 3710.

48  T. G. O'Lenick, X. Jiang and B. Zhao, *Langmuir*, 2010, **26**, 8787.

49  D. Park, W. Wu and Y. Wang, *Biomaterials*, 2011, **32**, 777.

50  M. J. Hwang, J. M. Suh, Y. H. Bae, S. W. Kim and B. Jeong, *Biomacromolecules*, 2005, **6**, 885.

51  W. Wang, L. Chang, X. Li, Y. Wu, J. Xing, L. Deng and A. Dong, *Soft Matter*, 2012, **8**, 1575.

52  R. Verber, A. Blanazs and S. P. Armes, *Soft Matter*, 2012, **8**, 9915.